Induction of growth inhibition and G_1 arrest in human cancer cell lines by relatively low-toxic diamantane derivatives

Jane-Jen Wang[a], Kuo-Tong Huang[b] and Yaw-Terng Chern[c]

We describe the discovery of a novel series of antitumor diamantane derivatives which induces G_1 arrest in Colo 205 cells. Eight diamantane derivatives were screened for their activity *in vitro* against 60 human cancer cell lines in the National Cancer Institute (NCI)'s anticancer drug screen. The relationships between structure and *in vitro* antitumor activity are discussed. The structure–activity relationship (SAR) study of diamantane derivatives clarified that the conformation of 1,6-bis(4-(4-aminophenoxy)-phenyl)diamantane (1,6-DPDONH$_2$) was essential for significant antitumor activity. Very strong growth inhibition of 1,6-DPDONH$_2$ (NSC-706829) was observed against one colon cancer line (Colo 205), four melanoma lines (MALME-3M, M14, SK-MEL-5 and UACC-257) and two breast cancer lines (MDA-MB-435 and MDA-N) with GI_{50} $<1.0\,\mu M$, i.e. below 0.01, 0.23, 0.48, 0.5, 0.32, 0.26 and $0.28\,\mu M$, respectively. 1,6-DPDONH$_2$ also exhibited particular selectivity against one colon cancer line (Colo 205), four melanoma lines (MALME-3M, M14, SK-MEL-5 and UACC-257) and two breast cancer lines (MAD-MB-435 and MDA-N) with $GI_{50} \leq 0.5\,\mu M$. In the same cancer subpanel, the selectivity of 1,6-DPDONH$_2$ between these seven most sensitive lines and the least sensitive line ranged from 40- to 100-fold. With the exception of melanoma lines, 1,6-bis(4-(4-amino-3-hydroxyphenoxy)-phenyl)diamantane (1,6-DPD/OH/NH$_2$) (NSC-706831) possessed stronger activity than 1,6-DPDONH$_2$ against almost all tested cancer lines. Very strong growth inhibition of 1,6-DPD/OH/NH$_2$ was observed against one leukemia line (HL-60(TB)), one NSCLC line (HOP-92), one ovarian cancer line (OVCAR-8) and one breast cancer line (T-47D) with GI_{50} $<1.0\,\mu M$, i.e. 0.50, 0.85, 0.62 and $0.75\,\mu M$, respectively. *Anti-Cancer Drugs* 15:277–286 © 2004 Lippincott Williams & Wilkins.

Anti-Cancer Drugs 2004, **15**:277–286

Keywords: antitumor activities, diamantane, G_1 arrest

[a]National Taipei College of Nursing and [b]Department of Internal Medicine, National Taiwan University Hospital, Taipei, Taiwan and [c]Department of Chemical Engineering, National Taiwan University of Science and Technology, Taipei Taiwan.

Correspondence to Y.-T. Chern, Department of Chemical Engineering, National Taiwan University of Science and Technology, 43, Keelung Road, Section 4, Taipei 106, Taiwan.
Tel: + 886 27376646; fax: + 886 27376644;
e-mail: cyt@ch.ntust.edu.tw

Received 27 May 2003 **Revised form accepted** 21 November 2003

Introduction

Adamantane derivatives possess several attractive pharmacological activities, such as antibacterial, antifungal, antiviral and anticancer effects [1–4]. Therefore, many investigators consider them as highly promising candidates in drug design [5–7]. For example, the aminoadamantane derivatives memantine (1-amino-3,5-dimethyladamantane) and amantadine (1-aminoadamantane) are uncompetitive *N*-methyl-D-aspartate (NMDA) receptor antagonists which have been used clinically in the treatment of dementia and Parkinson's disease for several years without serious side-effects [5,6]. Adamantane and diamantane are closely analogous polycyclic alkanes with the structure of three and six fused cyclohexane rings, respectively. Although diamantane derivatives have been investigated by chemists for many years, only a few studies of the biological activity of diamantane derivatives have been reported [8]. To the best of our knowledge, the present study is the first report that refers to the *in vitro* antitumor activities of diamantane derivatives.

Malignant tumor cells are clearly distinguished from normal cells by their chaotic proliferation due to a serious disorder of the cell-cycle regulatory machinery. Cell-cycle inhibitors or modulators that halt uncontrollable tumor growth are regarded as highly promising new therapeutic agents on human cancers [9]. Recent studies have shown that the G_1 phase of the cell cycle is an important period where various signals interact to determine the proliferation, quiescence, differentiation or apoptosis of cells [10,11].

In this study, we synthesized the diamantane derivatives, including 1,6-diaminodiamantane (1,6-DNH$_2$), 4,9-diaminodiamantane (4,9-DNH$_2$), 1,6-bis(4-aminophenyl)-diamantane (1,6-DPDNH$_2$), 4,9-bis(4-aminophenyl)-diamantane (4,9-DPDNH$_2$), 1,6-bis(4-(4-aminophenoxy)-phenyl)diamantane (1,6-DPDONH$_2$), 4,9-bis(4-(4-aminophenoxy)phenyl)diamantane (4,9-DPDONH$_2$), 1,6-bis(4-(4-amino-3-hydroxyphenoxy)phenyl)diamantane (1,6-DPD/OH/NH$_2$) and 1,6-bis(4-(4-amino-2-trifluoromethylphenoxy)phenyl)diamantane. The *in vitro* antitumor activities of those compounds were screened against the National Cancer Institute (NCI)'s 60 human cancer cell lines. In addition, we characterized the cell growth inhibition and cell-cycle progression by 1,6-DPD/OH/NH$_2$ in Colo 205 colon cancer cells. We also evaluated the acute toxicity of 1,6-DPDONH$_2$ in BALB/c mice.

0959-4973 DOI: 10.1097/01.cad.0000119453.84063.de

Materials and methods

Materials

1,6-Bis(4-hydroxyphenyl)diamantane was synthesized from 1,6-dibromodiamantane and phenol according to our previous method [12]. 1,6-DNH_2 [13], 4,9-DNH_2 [14], 1,6-$DPDNH_2$ [15], 4,9-$DPDNH_2$ [16], 1,6-$DPDONH_2$ [12], 4,9-$DPDONH_2$ [17] and 1,6-DPD/OH/NH_2 (unpublished data) were synthesized according to our previous methods.

General methods

A Bio-Rad FTS-40 FTIR spectrophotometer was used to record spectra of the KBr pellets. MS spectra were obtained using a JEOL DMS-D300 mass spectrometer. ^{1}H- and ^{13}C-NMR spectra were recorded on a Bruker AM-400 Fourier transform nuclear magnetic resonance spectrometer using tetramethyl silane (TMS) as the internal standard. A Perkin-Elmer 240C elemental analyzer was used for the elemental analysis.

Synthesis of 1,6-bis(4-(4-nitro-2-trifluoromethyl-phenoxy)phenyl)diamantane

A mixture of 1,6-bis(4-hydroxyphenyl)diamantane (1.80 g, 4.84 mmol), 2-chloro-5-nitrobenzotrifluoride (2.30 g, 10.2 mmol), potassium carbonate (1.60 g, 11.6 mmol) and 35 ml of dry *N*,*N*-dimethylformamide (DMF) was refluxed at 160°C for 12 h under nitrogen. The reaction mixture was allowed to cool to room temperature and then poured into distilled water. The precipitate was collected by filtration to afford 2.51 g (69.15%) of pale yellow crystals: m.p. > 380°C; IR(KBr) 3065, 2890, 2864, 1538, 1496, 1345 cm^{-1}; MS (EI) *m*/*z* 750 (M^+, 100), 296 (82); ^{1}H-NMR (400 MHz, $CDCl_3$) δ 1.55–1.60 (m, 8H, H-3a, 5, 8a; 10a, 13, 14a), 1.62 (brs, 2H, H-4,9), 1.95 (d, J = 12.6 Hz, 4H, H-3e, 8e, 10e, 14e), 2.60 (brs, 4H, H-2, 7, 11, 12), 6.98 (d, J = 9.2 Hz, 2H, H-c), 7.09 (d, J = 8.64 Hz, 4H, H-b), 7.48 (d, J = 8.8 Hz, 4H, H-a), 8.29 (m, 2H, H-d), 8.57 (s, 2H, H-e); anal. calcd for $C_{40}H_{32}F_6N_2O_6$: C, 64.0; H, 4.27; N, 3.73; found: C, 63.96; H, 4.30; N, 3.71.

Synthesis of 1,6-bis(4-(4-amino-2-trifluoromethyl-phenoxy)phenyl)diamantane (1,6-DPD/CF_3/NH_2)

A 150-ml, three-necked, round-bottomed flask was charged with 1,6-bis(4-(4-nitro-2-trifluoromethylphenoxy)-phenyl)diamantane (2.00 g, 2.67 mmol), 100 ml of ethanol, 100 ml of tetrahydrofuran and 0.12 g of 10% palladium on carbon (Pd-C). The mixture was heated to reflux and hydrazine monohydrate (60 ml) was added dropwise to the mixture. After a further 72 h reflux, the catalyst was removed by hot filtration. The filtrate was poured into 50 ml of water to give 1.72 g (93.3%) of off-white powder. The diamine (1,6-DPD/CF_3/NH_2) was purified by vacuum sublimation. m.p. > 350°C; IR(KBr) 3465, 3373, 3072, 2891, 2864, 1610, 1502 cm^{-1}; MS (EI) *m*/*z* 690 (M^+, 100), 345 (95), 176 (100); ^{1}H-NMR(400 MHz, DMSO-d_6) δ 1.45–1.49 (m, 8H, H-3a, 5, 8a; 10a, 13, 14a), 1.68 (s, 2H, H-4,9), 1.79 (d, J = 11.6 Hz, 4H, H-3e, 8e, 10e, 14e), 2.50 (s, 4H, H-2, 7, 11, 12), 5.42 (s, 4H,NH_2), 6.78–6.90 (m, 10H, H-c, f, g, i), 7.33 (d, J = 8.4 Hz, 4H, H-b); ^{13}C-NMR (100 MHz, DMSO-d_6) δ 27.36 (C-4, 9), 32.70 (C-3, 8, 10, 14), 38.29 (C-2, 7, 11, 12), 40.65 (C-1, 6), 49.44 (C-5, 13), 110.56 (C-f), 116.62 (C-c), 118.58 (C-i) 122.83 (C-g), 126.57 (C-b), 120.73, 121.02, 121.32, 121.61 (q, C-j), 122.82, 124.89, 126.75, 128.81 (q, CF_3), 142.60 (C-h),142.75 (C-e), 145.44 (C-a), 155.57 (C-d); anal. calcd for $C_{40}H_{36}F_6N_2O_2$: C, 69.56; H, 5.22; N, 4.06; found: C, 69.48; H, 5.24; N, 3.97.

Scheme 1

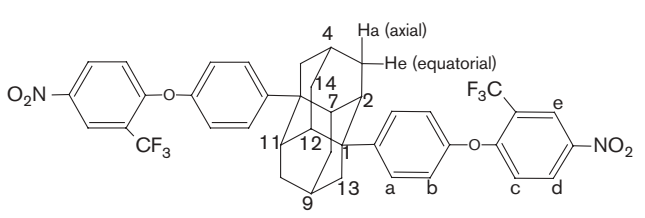

Scheme 2

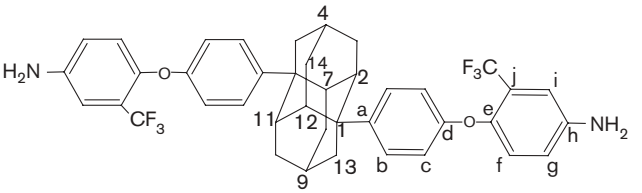

The NCI's anticancer drug screen

A total of 60 human cancer cell lines were used for the NCI's anticancer drug screen, including the subpanels of leukemia, melanoma, and cancers of lung, colon, brain, ovary, renal, breast and prostate. These cell lines were adaptable to a single growth medium, and had reproducible profiles for growth and drug sensitivity. The detailed methods are described in the literature [18].

Cell culture and 1,6-DPD/OH/NH_2 treatments

Colo 205 cells (ATCC: CCL-222) were cultured in RPMI 1640 with 10% fetal bovine serum (Hyclone, Logan, UT). Cells were incubated in a humidified atmosphere of 5% CO_2 in air at 37°C. 1,6-DPD/OH/NH_2 was dissolved in DMSO at a stock concentration of 10 mM and added to culture media at a final concentration of 0.1, 1 and 10 μM. Cells were seeded at 6×10^5 cells/60-mm or 1×10^6 cells/100-mm dish in growth medium. The following day the cells were replenished with medium containing the 1,6-DPD/OH/NH_2. Cells were harvested and counted by a hemocytometer at 24, 48 and 72 h after treatment with 1,6-DPD/OH/NH_2, and used for further analysis.

Analysis of the reversibility of 1,6-DPD/OH/NH_2-induced cycle arrest of Colo 205 cells

Cells (1×10^6/dish) were seeded on a 10-cm dish and allowed to attach overnight, and then the medium was discarded and replenished with medium containing the 1,6-DPD/OH/NH_2 for incubation at 37°C for 3 days. At the end of 3 days, the media was discarded and the cells were replenished with fresh medium. Cells were harvested, and the cell-cycle progression analyzed by flow cytometry at day 3, 4 and 5 after withdrawal from 1, 2 or 4 μM 1,6-DPD/OH/NH_2 reatment for 72 h.

DNA staining

The Cycle TEST Plus DNA Reagent Kit (Becton Dickinson, San Jose, CA) was used for DNA staining. After washing the cells twice with Buffer Solution, the cell concentration was adjusted to 1.0×10^6/ml and 0.5 ml of cell suspension was centrifuged at 400 *g* for 5 min at room temperature (20–25°C). The cell pellet was added to 250 μl of Solution A (trypsin buffer) and gently mixed. After incubation at room temperature for 10 min, 200 μl of Solution B (trypsin inhibitor and RNase buffer) was added to each tube, gently mixed and then incubated at room temperature for 10 min.This was followed by the addition of 200 μl of Solution C (propidium iodide stain solution) and incubated for 10 min in the dark on ice (2–8°C). The sample was filtered through a 50-mm nylon mesh and used for flow cytometric analysis.

Cells (20 000) were analyzed on a FACSCalibur flow cytometer (Becton Dickinson) using an argon-ion laser (15 mW) with the incident beam at 488 nm. The red fluorescence (propidium iodide) was collected through a 585-nm filter. The data were analyzed using ModFit and Cellquest software on a Macintosh computer.

Acute toxicity of 1,6-$DPDONH_2$ in BALB/c mice

The 8-week-old female and male BALB/c mice were obtained from the National Laboratory Animal Center of National Applied Research Laboratories (Taipei, Taiwan), and housed under conditions with the temperature maintained at 25°C and light controlled at a 12 h light/12 h dark cycle. 1,6-$DPDONH_2$ was dissolved in olive oil; treatment started when the body weight of the mice was 17–25 g. 1,6-$DPDONH_2$ was administered as a single dose via oral or i.p. injection at doses of 5 or 2 g/kg (volume of injection: 0.25 or 0.1 ml/10 g of body weight), respectively. The control group received olive oil vehicle. The body weight was monitored every 3–4 days throughout the experiment. ALT, AST and BUN were measured by the National Taiwan University Hospital's clinical biochemical laboratory (Taipei, Taiwan) at the end of the experiment. At day 14, all mice were sacrificed by CO_2 gas. The livers, kidneys and lungs were collected, fixed, embedded and stained with hematoxylin & eosin for pathological analysis.

Statistics

All data are expressed as mean ± SE. Difference between groups was assessed using Student's *t*-test. A $p < 0.05$ is considered as a significant difference.

Results and discussion

Chemistry

In order to systematically evaluate the structure–activity relationship (SAR) study of diamantane derivatives, eight diamantane derivatives were synthesized. A novel 1,6-DPD/CF_3/NH_2 was synthesized from 1,6-bis(4-hydroxyphenyl)diamantane in two steps. Reaction of 1,6-bis(4-hydroxyphenyl)diamantane with 2-chloro-5-nitrobenzotrifluoride in anhydrous DMF in the presence of potassium carbonate as an acid acceptor gave 1,6-bis(4-(4-nitro-2-trifluoromethylphenoxy)phenyl)diamantane, which was hydrogenated to give 1,6-DPD/CF_3/NH_2. We noted that the hydrogenation of the nitro compound bearing strong electron-withdrawing substituents (CF_3) is relatively difficult. More catalyst (Pd-C) and reaction time were necessary for the hydrogenation of 1,6-DPD/CF_3/NO_2. When the nitro compound was converted into 1,6-DPD/CF_3/NH_2, the signal in ^{1}H-NMR appearing at 5.42 p.p.m. is peculiar to the amino group. In addition, results obtained from the elemental analysis, characteristic peaks in the NMR spectra and characteristic bands in the IR spectra confirmed the structures of 1,6-DPD/CF_3/NH_2.

SARs of diamantane derivatives

For comparison of antitumor activities of the diamantane derivatives, the 1,6-(1,6-DNH_2, 1,6-$DPDNH_2$ and 1,6-$DPDONH_2$) and 4,9-(4,9-DNH_2, 4,9-$DPDNH_2$ and 4,9-$DPDONH_2$) substituted diamantane derivatives were synthesized (Fig. 1). Table 1 shows the comparison of *in vitro* antitumor activities of the diamantane derivatives against the three cancer cell lines. Only 1,6-$DPDONH_2$ exhibited modest growth inhibitory activities against the three cancer cell lines. However, 4,9-$DPDONH_2$, 1,6-$DPDNH_2$, 4,9-$DPDNH_2$, 1,6-DNH_2 and 4,9-DNH_2 were virtually inactive. Comparison of the antitumor activities of 1,6-$DPDONH_2$ and 4,9-$DPDONH_2$ indicated that 4,9-$DPDONH_2$ was virtually inactive *in vitro* against the NCI's 60 human cancer cell lines. 1,6-$DPDONH_2$ and 4,9-$DPDONH_2$ have a similar chemical structure (amine functional groups and diamantane backbone units). However, they have very different antitumor activity. For example, very strong growth inhibition of 1,6-$DPDONH_2$ was observed against one colon cancer line (Colo 205), four melanoma lines (MALME-3M, M14, SK-MEL-5 and UACC-257) and two breast cancer lines (MDA-MB-435 and MDA-N) with $GI_{50} < 1.0$ μM, i.e. below 0.01, 0.23, 0.48, 0.5, 0.32, 0.26 and 0.28 μM, respectively (see Table 2). The results suggest that the configuration of 1,6-$DPDONH_2$ plays a prominent role in their antitumor activities. We noted that the base moiety of 1,6-$DPDONH_2$ is a potential anticancer agent.

Fig. 1

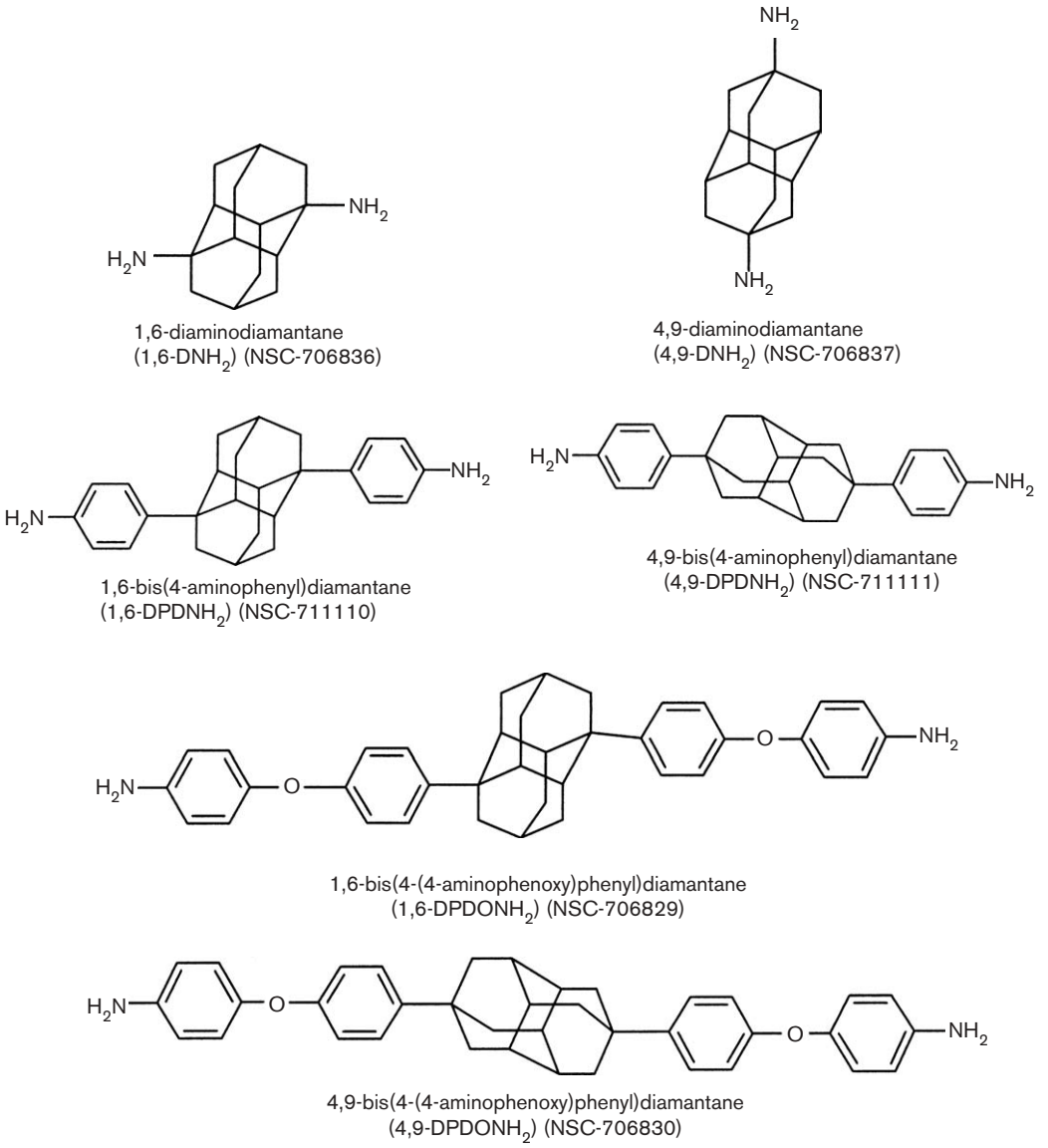

Chemical structures of diamantane derivatives.

Table 1 ***In vitro*** **antitumor activities of the diamantane derivatives**

Compounds	GI50(μM)		
	NCI-H460 (lung cancer)	MCF7 (breast cancer)	SF-268 (CNS cancer)
1,6-DPDONH$_2$	25.9	37.0	37.7
4,9-DPDONH$_2$	>100	>100	>100
1,6-DPDNH$_2$	>100	>100	>100
4,9-DPDNH$_2$	>100	>100	>100
1,6-DNH$_2$	>100	>100	>100
4,9-DNH$_2$	>100	>100	>100
1,6-DPD/CF$_3$/NH$_2$	>100	>100	>100
1,6-DPD/OH/NH$_2$	4.21	5.07	4.37

The antitumor activities of 1,6-DPDONH$_2$

1,6-DPDONH$_2$ was tested for its antitumor activity at five concentrations, i.e. 10^{-4}, 10^{-5}, 10^{-6}, 10^{-7} and 10^{-8} M. The values of GI_{50} (50% growth inhibition), total growth inhibition (TGI) and LC_{50} (50% cell killing) are summarized in Table 2.

As shown in Table 2, 1,6-DPDONH$_2$ exhibited growth inhibition against almost all the test cells from leukemia and solid tumors with $GI_{50} < 100\,\mu M$. Very strong growth inhibition was observed against one colon cancer line

Table 2 The antitumor activities of 1,6-bis(4-(4-aminophenoxy)-phenyl)diamantine (NSC-706829)

Panel/cell line	GI_{50} (μM)	TGI (μM)	LC_{50} (μM)
Leukemia			
CCRF-CEM	13.1	>100	>100
HL-60(TB)	4.76	19.7	90.7
K-562	7.28	42.1	>100
MOLT-4	5.52	27.4	>100
RPMI-8226	8.89	30.5	>100
NSCLC			
A549/ATCC	11.3	>100	>100
EKVX	6.81	>100	>100
HOP-62	14.3	51.3	>100
HOP-92	2.1	7.54	>100
NCI-H226	25.8	95.7	>100
NCI-H23	36.7	>100	>100
NCI-H322M	12	>100	>100
NCI-H460	25.9	84.6	>100
NCI-H522	13.6	66.6	>100
Colon cancer			
Colo 205	<0.01	<0.01	0.37
HCT-116	6.38	54.7	>100
HCT-15	20.8	>100	>100
HT29	9.27	>100	>100
KM12	14.1	>100	>100
SW-620	18.2	>100	>100
CNS cancer			
SF-268	37.3	>100	>100
SF-295	21	79.4	>100
SNB-19	12.7	>100	>100
U251	2.91	14.9	45.9
Melanoma			
LOX IMVI	19.4	>100	>100
MALME-3M	0.23	11.6	72.8
M14	0.48	27.4	>100
SK-MEL-2	4.33	30.3	>100
SK-MEL-28	1.13	>100	>100
SK-MEL-5	0.5	2.72	17.3
UACC-257	0.32	>100	>100
UACC-62	2.54	>100	>100
Ovarian cancer			
IGROV1	26.2	>100	>100
OVCAR-3	6.5	29.7	>100
OVCAR-4	5.3	>100	>100
OVCAR-5	>100	>100	>100
OVCAR-8	36.2	>100	>100
Renal cancer			
786-0	11.9	64	>100
A498	22.2	66	>100
ACHN	2.87	>100	>100
CAKI-1	16.9	56	>100
RXF-393	21.9	71.6	>100
SN12C	15.9	>100	>100
TK-10	37.2	>100	>100
UO-31	3.79	>100	>100
Prostate cancer			
PC-3	5.22	65.5	>100
DU-145	8.92	>100	>100
Breast cancer			
MCF-7	37	>100	>100
NCI/ADR-RES	>100	>100	>100
MDA-MB-231	9.08	65.7	>100
HS 578T	39.3	>100	>100
MDA-MB-435	0.26	15.4	>100
MDA-N	0.28	22.4	>100
BT-549	40.7	>100	>100
T-47D	8.5	>100	>100

(Colo 205), five melanoma lines (MALME-3M, M14, SK-MEL-28, SK-MEL-5 and UACC-257) and two breast cancer lines (MDA-MB-435 and MDA-N) with $GI_{50} \leq 2.0\,\mu M$, i.e. below 0.01, 0.23, 0.48, 1.13, 0.5, 0.32, 0.26 and 0.28 μM, respectively. 1,6-$DPDONH_2$ also exhibited moderate growth inhibition against four leukemia lines (HL-60(TB), MOLT-4, RPMT-8226 and K-562), two NSCLC lines (EKVX and HOP-92), two colon cancer lines (HCT-116 and HT29), one CNS cancer line (U251), two melanoma lines (SK-MEL-2 and UACC-62), two ovarian cancer lines (OVCAR-3 and OVCAR-4), two renal cancer lines (ACHN and UO-31), two prostate cancer lines (PC-3 and DU-145) and two breast cancer lines (MDA-MB-231 and T-47D) with GI_{50} from 2 to 10 μM, i.e. 4.76, 5.52, 8.89, 7.28, 6.81, 2.1, 6.38, 9.27, 2.91, 4.33, 2.54, 6.5, 5.3, 2.87, 3.79, 5.22, 8.92, 9.08 and 8.5 μM, respectively. In the same cancer subpanel, selectivity more than 100-fold is observed between Colo 205 and HCT-116, HCT-15, HT29, KM12 and SW-620 in colon cancer. In addition, selectivity more than 40-fold is observed between LOX IMVI and MALME-3M, M14, SK-MEL-5 and UACC-257 in melanoma cancer.

In vitro antitumor activity of 1,6-substituted diamantane derivatives

To further confirm that the substituted groups of 1,6-substituted diamantane derivatives affect the growth inhibition of cancer cells. 1,6-$DPD/CF_3/NH_2$ and 1,6-$DPD/OH/NH_2$ were synthesized (Fig. 2). Comparison of the antitumor activities of 1,6-$DPDONH_2$ and 1,6-$DPD/CF_3/NH_2$ indicated that 1,6-$DPD/CF_3/NH_2$ was virtually inactive *in vitro* against the three cancer lines (Table 1). 1,6-$DPDONH_2$ and 1,6-$DPD/CF_3/NH_2$ have similar chemical structures (amine functional groups and diamantane backbone units). However, they have very different antitumor activity. It is likely that the configurations of 1,6-$DPDONH_2$ play a prominent role in their antitumor activities. This result suggested that structure **I** (Fig. 2) was essential for significant antitumor activity. The subsequent synthetic transformations of 1,6-$DPDONH_2$ to 1,6-$DPD/OH/NH_2$ led to a remarked enhancement of antitumor activity toward the three cancer lines (Table 1). The role of the OH group at the *ortho* position of the NH_2 on growth inhibition is remarkable. In addition, 1,6-$DPD/OH/NH_2$ remains in the configuration of 1,6-$DPDONH_2$ because the OH group is at the *meta* position of ether unit. In other words, 1,6-$DPDONH_2$ and 1,6-$DPD/OH/NH_2$ have similar conformations. The result also suggested that the structure **I** may function as the active core.

The antitumor activities of 1,6-$DPD/OH/NH_2$

1,6-$DPD/OH/NH_2$ was screened for its activity *in vitro* against 60 human cancer cell lines in the NCI's *in vitro* anticancer drug screen by the SRB assay. The values of GI_{50} and LC_{50} are summarized in Table 3. As shown in Table 3, 1,6-$DPD/OH/NH_2$ exhibited growth inhibition against almost all the test cells from leukemia and solid tumors with $GI_{50} < 100\,\mu M$. Very strong growth inhibition was observed against one leukemia line (HL-60(TB)), one NSCLC line (HOP-92), one ovarian cancer line (OVCAR-8) and one breast cancer line (T-47D) with

Fig. 2

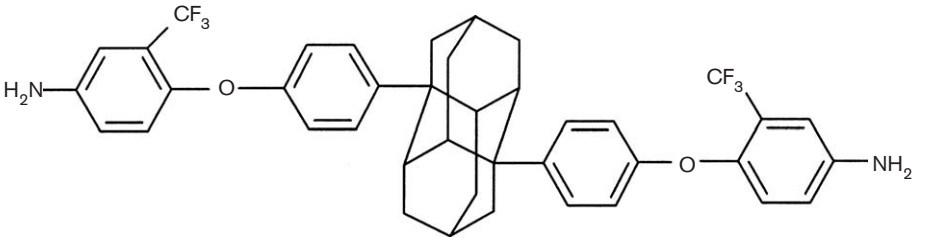

1,6-bis(4-(4-amino-2-trifluromethylphenoxy)phenyl)diamantane
(1,6-DPD/CF_3/NH_2) (NSC-711112)

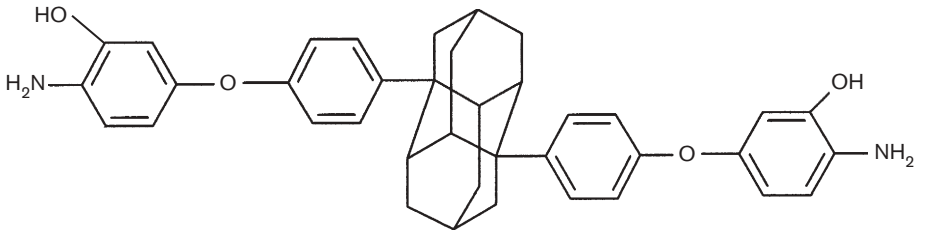

1,6-bis(4-(4-amino-3-hydrophenoxy)phenyl)diamantane
(1,6-DPD/OH/$NH)_2$ (NSC-706831)

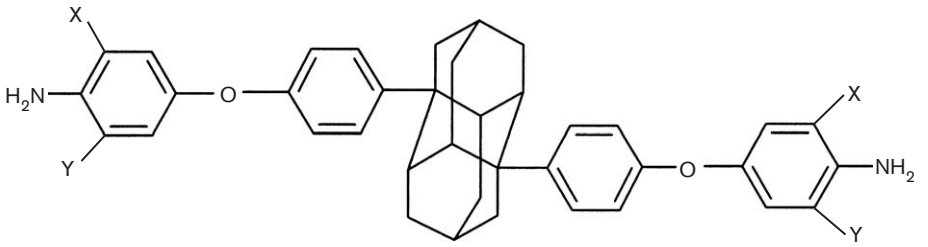

Structure **I**

Chemical structures of the 1,6-substituted diamantane derivatives.

GI_{50} < 1.0 μM, i.e. 0.50, 0.85, 0.62 and 0.75 μM, respectively. 1,6-DPD/OH/NH_2 also exhibited moderate growth inhibition against almost tested cancer lines with GI_{50} from 1 to 10 μM. The data of response parameters in Table 3 can be plotted by the NCI's mean graph as shown in Fig. 3. The mean graph facilitates visual scanning of data for potential patterns of selectivity for particular cell lines or for particular subpanels with respect to a selected response parameters. The mean graph shows the pattern at each of the principal response parameters, i.e. GI_{50}, TGI and LC_{50}. The vertical line of each response parameter group represents the mean value of all test data against cell lines. Therefore, bars extending to the right represent sensitivity of the cell line in excess of the average sensitivity of all cell lines. Bars extending to the left imply sensitivity of the cell line less than the average sensitivity. The bars of those $\log_{10}GI_{50} < 5.7$ (i.e. GI_{50} < 1.0 μM in Table 3) extending to the right by approximately 0.6 include HL-60(TB), HOP-92, OVCAR-8 and T-47D cell lines from four subpanels, suggesting the responses against these cell lines are more selective than other lines. However, selectivity was almost less than 10-fold in the same cancer subpanel.

Comparison of antitumor activities of 1,6-DPDONH_2 and 1,6-DPD/OH/NH_2

Comparison of antitumor activities of 1,6-DPDONH_2 and 1,6-DPD/OH/NH_2 indicated that 1,6-DPD/OH/NH_2 possessed stronger activity against almost tested cancer lines with the exception of melanoma lines (Tables 2 and 3). However, 1,6-DPD/OH/NH_2 is remarkably weaker than 1,6-DPDONH_2 in inhibiting particular cell lines such as Colo 205 and melanoma. The reason for the relatively strong growth inhibition against the melanoma cell lines for 1,6-DPDONH_2 is not clear. Further experiments will be performed in the future. In the same cancer subpanel, at the GI_{50} level, selectivity of 1,6-DPDONH_2 is notably higher than that of 1,6-DPD/OH/NH_2 in colon, breast cancer and melanoma cancer lines.

Table 3 The antitumor activities of 1,6-bis(4-(4-amino-3-hydroxyphenoxy)phenyl)diamantine (NSC-706831)

Panel/cell line	GI_{50} (μM)	TGI (μM)	LC_{50} (μM)
Leukemia			
CCRF-CEM	2.36	17.0	>100
HL-60(TB)	0.50	3.27	>100
K-562	2.78	>100	>100
MOLT-4	2.21	14.9	>100
RPMI-8226	1.92	7.75	>100
NSCLC			
A549/ATCC	2.71	21.2	>100
EKVX	2.58	62.6	>100
HOP-62	2.34	14.6	48.3
HOP-92	0.85	4.69	22.3
NCI-H226	4.18	15.9	46.9
NCI-H23	4.48	19.8	72.3
NCI-H322M	3.99	>100	>100
NCI-H460	4.21	>100	>100
NCI-H522	1.71	5.45	51.0
Colon cancer			
Colo 205	1.31	2.85	6.24
HCT-116	1.99	12.6	79.4
HCT-15	3.51	25.2	>100
HT29	3.56	>100	>100
KM12	3.61	28.6	>100
SW-620	4.40	30.0	>100
CNS cancer			
SF-268	4.37	25.3	>100
SF-295	2.47	13.7	42.3
SNB-19	7.53	26.9	79.8
U251	2.57	13.6	50.5
Melanoma			
LOX IMVI	2.93	12.2	48.3
MALME-3M	12.0	27.6	63.5
M14	3.01	18.4	>100
SK-MEL-2	21.7	45.7	96.3
SK-MEL-28	10.1	24.1	57.8
SK-MEL-5	2.45	6.19	26.1
UACC-257	5.13	85.6	>100
UACC-62	11.9	33.2	93.0
Ovarian cancer			
IGROV1	4.89	19.3	66.2
OVCAR-3	1.47	8.28	34.6
OVCAR-4	3.74	22.9	89.6
OVCAR-5	3.65	>100	>100
OVCAR-8	0.62	21.9	>100
Renal cancer			
786-0	3.19	16.1	59.2
A498	7.64	21.0	49.4
ACHN	2.80	14.8	46.7
CAKI-1	5.02	49.1	>100
RXF-393	6.61	30.2	>100
SN12C	6.20	9.73	58.9
TK-10	7.61	24.3	67.7
UO-31	4.59	21.0	82.7
Prostate cancer			
PC-3	1.93	13.8	78.3
DU-145	6.95	>100	>100
Breast cancer			
MCF-7	5.07	>100	>100
NCI/ADR-RES	3.69	86.2	>100
MDA-MB-231	3.75	14.9	>100
HS 578T	14.4	75.0	>100
MDA-MB-435	3.26	16.5	59.8
MDA-N	3.59	17.5	81.2
BT-549	2.93	26.8	>100
T-47D	0.75	>100	>100

Flow cytometric analysis

The cell-cycle progression of Colo 205 cells was examined using flow cytometry after exposure to 0.5, 1, 2 or 4 μM 1,6-DPD/OH/NH_2 for 24–72 h. Figure 4(A) shows that the majority of Colo 205 cells accumulated in the G_1 phase (89%) with a decrease of cells in the S (8.1%) and G_2/M (2.9%) phase after treatment with 1 μM 1,6-DPD/OH/NH_2 for 48 h. Colo 205 cells were mainly in G_0/G_1 phase (87.1-94%), and only a few percent of cells in the S (2.1–10.3%) and G_2/M (2.7–4.3%) phase after exposure to 2 or 4 μM 1,6-DPD/OH/NH_2 for 24–72 h. These results showed that treatment of colon cancer cells with 1,6-DPD/OH/NH_2 resulted in increased G_0/G_1 phase with a concomitant decrease of cells in the S and G_2/M phase. From this result, 1,6-DPD/OH/NH_2 exhibited a potent G_1 arrest in Colo 205 cells in a dose-dependent manner. Compared with other G_1 arresting compounds, there are no similar structures to that of 1,6-DPD/OH/NH_2. The targets and action mechanism of 1,6-DPD/OH/NH_2-induced G_1 arrest will be further studied. Table 4 shows that majority of Colo 205 cells accumulated in the G_1 phase (78–86%) with a decrease of cells in the S phase (4.6–13.6%) after treatment with 1–10 μM 1,6-DPDONH_2 for 24–72 h. The results also suggest that 1,6-DPDONH_2 induces G_1 arrest in Colo 205 cells. Those phenomena are similar for 1,6-DPDONH_2 and 1,6-DPD/OH/NH_2 because the structure and the mechanism of inhibition may be essentially the same. The results also suggested that structure **I** is the core structure for the antitumor activity.

The irreversible effect of 1,6-DPD/OH/NH_2-induced cycle arrest of Colo 205

To further investigate whether the 1,6-DPD/OH/NH_2-induced cycle arrest was reversible, Colo 205 cells were treated with 1,6-DPD/OH/NH_2 for 72 h and the cells were withdrawn from 1,6-DPD/OH/NH_2 by culturing in fresh medium for another 72, 96 or 120 h. As shown in Fig. 4(B) at 120 h after removal of 1 μM 1,6-DPD/OH/NH_2 from the medium, the cycle arrest of Colo 205 was reversed and returned to the control level. However, no reversal effect was observed after 2 or 4 μM 1,6-DPD/OH/NH_2 treatment and then withdrawal for 120 h. The population of sub-G_0/G_1 cells was not observed on 1,6-DPD/OH/NH_2-treated cells, except the cells after 4 μM 1,6-DPD/OH/NH_2 treatment then withdrawal for 120 h (8.76%). These results highlight the important properties of the irreversible differentiation effect of 1,6-DPD/OH/NH_2. One possibility is that the relatively lipophilic nature of 1,6-DPD/OH/NH_2 reduces cellular efflux upon rinsing of drug-containing medium after the initial drug exposure. The continued growth-inhibitory activity may be due to residual intracellular drug.

In vivo acute toxicity of single-dose challenge of 1,6-DPDONH_2

We further examined the *in vivo* acute toxicity of 1,6-DPDONH_2; female and male BALB/c mice were used. 1,6-DPDONH_2 was administered as single dose via oral or i.p. injection at doses of 5 or 2 g/kg (volume of injection: 0.25 or 0.1 ml/10 g of body weight), respectively. The doses were used according to the maximum

Fig. 3

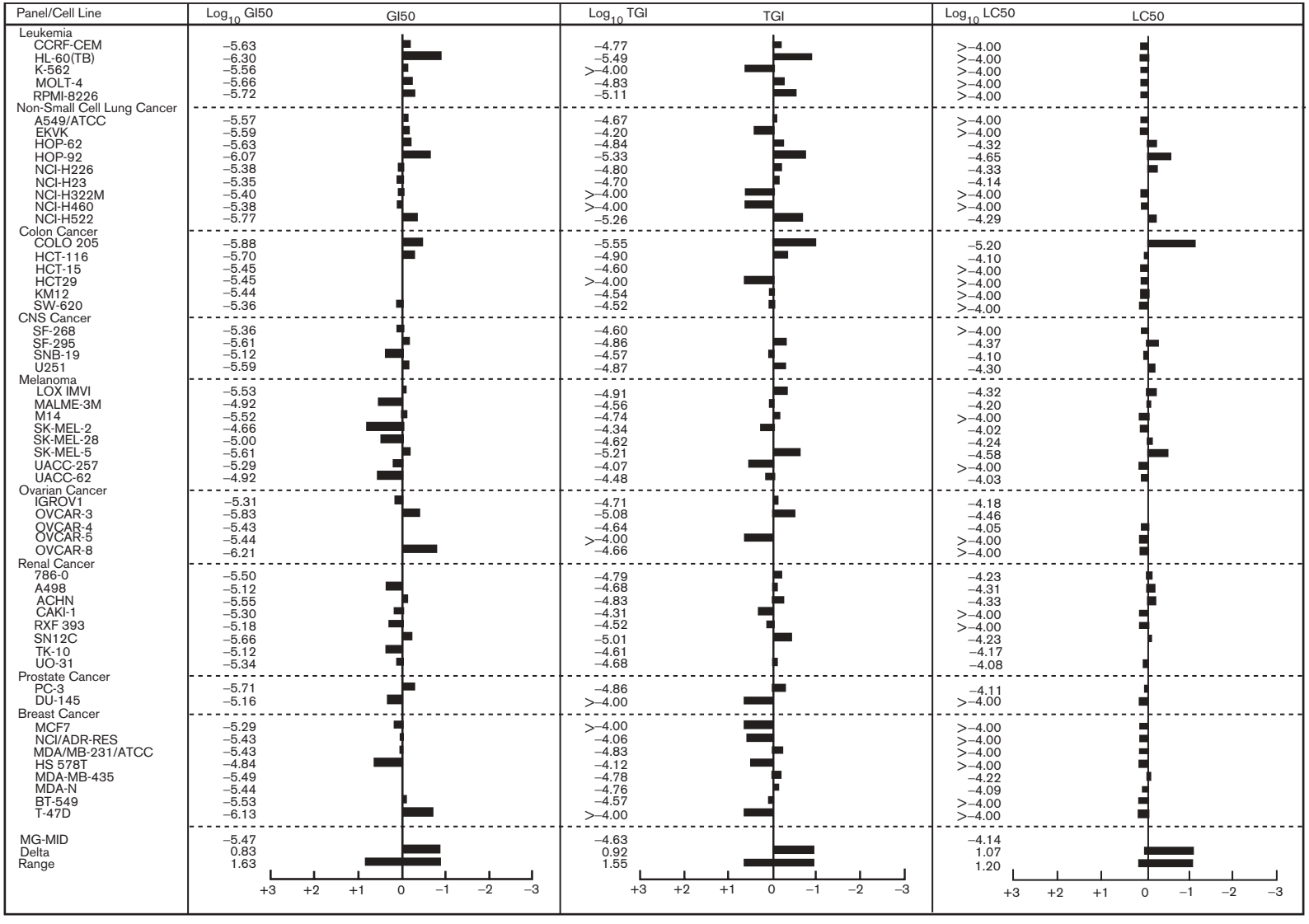

The mean graphs of 1,6-DPD/OH/NH_2 (NSC-706831) against the NCI's 60 human cancer cell lines.

Table 4 **Cell-cycle analysis of 1,6-DPDONH$_2$-treated Colo 205 cells**

Days	Phase of the cell cycle	1,6-DPDONH$_2$ (μM)			
		Vehicle	0.1	1	10
1	G_0/G_1	46.8	52.8	78.1	77.9
	S	38.5	35.8	13.6	12.7
	G_2/M	14.7	11.4	8.4	9.4
2	G_0/G_1	48.2	60.9	86.0	83.5
	S	39.3	29.0	4.6	8.7
	G_2/M	12.5	10.1	9.4	7.6
3	G_0/G_1	49.2	58.4	84.3	84.7
	S	43.2	32.0	6.1	7.0
	G_2/M	7.6	9.5	9.5	8.3

Fig. 4

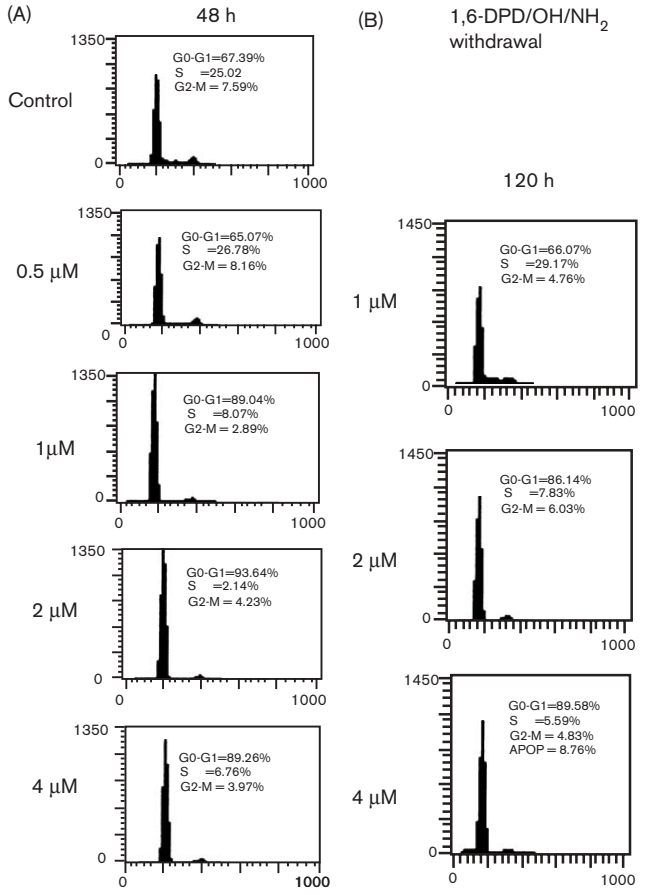

(A) The effect of 1,6-DPD/OH/NH$_2$ on cell-cycle arrest at 48 h in Colo 205 colon cancer cell lines. (B) The irreversible effect of 1,6-DPD/OH/NH$_2$-induced cycle arrest of Colo 205 Cells. Cells were harvested at 120 h after 1, 2 or 4 μM 1,6-DPD/OH/NH$_2$ treatment for 72 h, then withdrawal.

tolerated dose of the tested compound [19,20]. With treatment of BALB/c mice with single-dose 1,6-DPDONH$_2$ (5 g/kg; oral, 2 g/kg; i.p.), the body weight showed no significant ($P < 0.05$) reduction in both male and female mice as compared to control groups. In addition, liver and kidney function were as same as the control. Moreover, no tissue damage was observed in liver, lung and kidney after examination of the tissue slices stained with hematoxylin & eosin. These results showed the single-dose challenge of 1,6-DPDONH$_2$ in mice produced no obviously acute toxicity.

Disordered proliferation is one of the characteristics of most malignant tumors. Therefore, restoring normal cell-cycle control in tumor cells by using small molecule inhibitors of the cell cycle has been considered for anticancer chemotherapy. Recent studies have shown that the G_1 phase of the cell cycle is an important period where various signals interact to determine the proliferation, quiescence, differentiation or apoptosis of cells [10,11]. In the present study, we have demonstrated that 1,6-DPD/OH/NH$_2$ could mediate accumulation of Colo 205 cells in G_1 phase. Moreover, single-dose challenge of 1,6-DPDONH$_2$ in mice produced no obviously acute toxicity, indicating the possibility that 1,6-DPDONH$_2$ may be a promising candidate for clinical therapeutic protocols and merit further investigation. Therefore, the combination with other antineoplastic agents (e.g. a G_1-targeting agent [21]) in several different administration schedules will be further estimated in human colon cancer cells.

Conclusion

Herein we describe the *in vitro* antitumor and *in vivo* acute toxicity profile of 1,6-DPDONH$_2$. The SAR study of diamantane derivatives clarified that the conformation of 1,6-DPDONH$_2$ was essential for significant antitumor activity. Comparison of the growth inhibition of 1,6-DPDONH$_2$ and 1,6-DPD/OH/NH$_2$ indicated that 1,6-DPD/OH/NH$_2$ possessed stronger activity against almost all tested cancer lines with the exception of melanoma lines. However, 1,6-DPDONH$_2$ exhibited strong growth-inhibitory activity and high selectivity against the melanoma lines. In addition, 1,6-DPDONH$_2$ and 1,6-DPD/OH/NH$_2$ could mediate accumulation of Colo 205 cells in the G_1 phase. Moreover, single-dose challenge of 1,6-DPDONH$_2$ in mice produced no obviously acute toxicity, indicating the possibility that 1,6-DPDONH$_2$ may be a promising candidate for clinical therapeutic protocols and merit further investigation.

Acknowledgments

The authors are grateful to Drs Ven L. Narayanan, Edward Sausville, Yali F. Hallock, Anthony B. Mauger and Robert J. Schultz at the NCI for kind assistance. We are grateful to the National Science Council of the Republic of China for the support of this work.

References

1 Aigami K, Inamoto Y, Takaishi N, Hattori K. Biologically active polycycloalkanes. 1. Antiviral adamantine derivatives. *J Med Chem* 1975; **18**:713–721.

2 Tverdislov VA, el-Karadagi S, Kharitonenkov IG, Glaser R, Donath E, Herrmann A, *et al.* Interaction of the antivirus agents remantadine and

amantadine with lipid membranes and the influence on the curvature of human red cells. *Gen Physiol Biophys* 1986; **5**:61–75.
3 Chen HSV, Pellegrini JW, Aggarwal SK, Lei SZ, Warach S, Jensen FE, *et al.* Open-channel block of *N*-methyl-D-aspartate (NMDA) responses by memantine: therapeutic advantage against NMDA receptor-mediated neurotoxicity. *J Neurosci* 1992; **12**:4427–4436.
4 Wang JJ, Chern YT, Chang YF, Liu TY, Chi CW. Dimethyladamantylmaleimide-induced *in vitro* and *in vivo* growth inhibition of human colon cancer Colo 205 cells. *Anticancer Drugs* 2002; **13**:533–543.
5 Kornhuber J, Bormann J, Hubers M, Rusche K, Riederer P. Effects of the 1-amino-adamantanes at the MK-801-binding site of the NMDA-receptor-gated ion channel: a human postmortem brain study. *Eur J Pharmacol* 1991; **206**:297–300.
6 Donath E, Herrmann A, Coakley WT, Groth T, Egger M, Taeger M. The influence of the antiviral drugs amantadine and remantadine on erythrocyte and platelet membranes and its comparison with that of tetracaine. *Biochem Pharmacol* 1987; **36**:481–487.
7 Tsuzuki N, Hama T, Kawada M, Hasui A, Konishi R, Shiwa S, *et al.* Admantane as a brain-directed drug carrier for poorly absorbed drug. 2. AZT derivatives conjugated with the 1-admantane moiety. *J Pharmac Sci* 1994; **83**:481–484.
8 Chen CSH, Shen DM, Wentzek SE. Preparation of adamantane and diamantane derivatives as antivirals. *WO 9428885 Al*; 1994.
9 Hung DT, Jamison TF, Schreiber SL. Understanding and controlling the cell cycle with natural products. *Chem Biol* 1996; **3**:623–639.
10 Sherr CJ. Cancer cell cycles. *Science* 1996; **274**:1672–1677.
11 Sherr CJ. G_1 phase progression: cycling on cue. *Cell* 1994; **79**:551–555.
12 Chern YT. Low dielectric constants of soluble polyimides derived from novel 1,6-bis(4-(4-aminophenoxy)phenyl)diamantane. *Macromolecules* 1998; **31**:5837–5844.
13 Chern YT, Wang JJ. Synthesis of 1,6-diaminodiamantane. *Tetrahedron Lett* 1995; **36**:5805–5806.
14 Chern YT, Huang CM. Synthesis and characterization of new polyimides derived from 4,9-diaminodiamantane. *Polymer* 1998; **39**:6643–6648.
15 Chern YT. High subglass transitions appear in the rigid polyimides derived from novel 1,6-bis(4-aminophenyl)diamantane. *Macromolecules* 1998; **31**:1898–1905.
16 Chern YT, Shiue HC. High subglass transitions temperatures and low dielectric constants of polyimides derived from 4,9-bis(4-aminophenyl) diamantane. *Chem Mater* 1998; **10**:210–216.
17 Chern YT, Shiue HC. Low dielectric constants of soluble polyimides derived from novel 4,9-bis(4-(4-aminophenoxy)phenyl)diamantane. *Macromolecules* 1997; **30**:5766–5772.
18 Monga M, Sausville EA. Developmental therapeutics program at the NCI: molecular target and drug discovery process. *Leukemia* 2002; **16**:520–526.
19 OECD. Acute oral toxicity (401). In: *OCED Guidelines for Testing of Chemicals*. Paris: OECD; 1987.
20 Auletta CS. Acute, subchronic, and chronic toxicology. In: Derelanko MJ (editor): *CRC Handbook of Toxicology*, 3rd edn. Boca Raton, FL: CRC Press; 1995, pp. 51–104.
21 Takashi O, Hiroshi Y, Tatsuo O, Kentaro Y, Yoichi O, Naoko HS, *et al.* Discovery of novel antitumor sulfonamides targeting G_1 phase of the cell. *J Med Chem* 1999; **42**:3789–3799.